MIT Open Access Articles

Zero–group-velocity modes in chalcogenide holey photonic-crystal fibers

Massachusetts Institute of Technology

Zero–group-velocity modes in chalcogenide holey photonic-crystal fibers

Ardavan F. Oskooi,[1] **J. D. Joannopoulos,**[2] **and Steven G. Johnson**[3]

[1]*Center for Materials Science and Engineering,*
[2]*Department of Physics,* [3]*Department of Mathematics,*
Massachusetts Institute of Technology, 77 Massachusetts Ave., Cambridge MA 02139.
ardavan@mit.edu

Abstract: We demonstrate that a holey photonic-crystal fiber with chalcogenide-glass index contrast can be designed to have a complete gap at a propagation constant $\beta = 0$ that also extends into the non-zero β region. This type of bandgap (previously identified only at index contrasts unattainable in glasses) opens up a regime for guiding zero–group-velocity modes not possible in holey fibers with the more common finger-like gaps originating from $\beta \to \infty$. Such modes could be used to enhance nonlinear and other material interactions, such as for hollow-core fibers in gas-sensor applications.

References and links

1. P. Russell, "Photonic Crystal Fibers," Science **299**(5605), 358–362 (2003).
2. J. Pottage, D. Bird, T. Hedley, T. Birks, J. Knight, P. Russell, and P. Roberts, "Robust photonic band gaps for hollow core guidance in PCF made from high index glass," Opt. Express **11**, 2854–2861 (2003).
3. M. Ibanescu, S. G. Johnson, D. Roundy, C. Luo, Y. Fink, and J. D. Joannopoulos, "Anomalous Dispersion Relation by Symmetry Breaking in Axially Uniform Waveguides," Phys. Rev. Lett. **92**, 063,903 (2004).
4. X.-P. Feng and Y. Arawaka, "Off-plane angle dependence of photonic band gap in a two dimensional photonic crystal," IEEE J. Quantum Electron. **32**, 535–542 (1996).
5. R. Meade, K. Brommer, A. Rappe, and J. Joannopoulos, "Existence of a photonic band gap in two dimensions," Appl. Phys. Lett. **61**, 495–497 (1992).
6. J. Winn, R. Meade, and J. Joannopoulos, "Two-dimensional Photonic Band-gap Materials," J. Mod. Opt. **41**, 257–273 (1994).
7. A. Maradudin and A. McGurn, "Out of Plane Propagation of Electromagnetic Waves in a Two-dimensional Periodic Dielectric Medium," J. Mod. Opt. **41**, 275–284 (1994).
8. T. Haas, A. Hesse, and T. Doll, "Omnidirectional two-dimensional photonic crystal band gap structures," Phys. Rev. B **73**(045130) (2006).
9. G. Benoit and Y. Fink, "MIT electronic database of optical properties," `http://mit-pbg.mit.edu/Pages/DataBase.html` (2006).
10. J. Nishii, T. Yamashita, and T. Yamagishi, "Chalcogenide glass fiber with a core—cladding structure," Appl. Opt. **28**, 5122–5127 (1989).
11. T. Monro, Y. West, D. Hewak, N. Broderick, and D. Richardson, "Chalcogenide holey fibres," Electron. Lett. **36**, 1998–2000 (2000).
12. K. Kiang, K. Frampton, T. Monro, R. Moore, J. Tucknott, D. Hewak, D. Richardson, and H. Rutt, "Extruded singlemode non-silica glass holey optical fibres," Electron. Lett. **38**, 546–547 (2002).
13. V. V. R. K. Kumar, A. George, J. Knight, and P. Russell, "Tellurite photonic crystal fiber," Opt. Express **11**, 2641–2645 (2003).
14. L. Brilland, F. Smektala, G. Renversez, T. Chartier, J. Troles, T. Nguyen, N. Traynor, and A. Monteville, "Fabrication of complex structures of Holey Fibers in Chalcogenide glass," Opt. Express **14**, 1280–1285 (2006).

15. J. L. Person, F. Smektala, T. Chartier, L. Brilland, T. Jouan, J. Troles, and D. Bosc, "Light guidance in new chalcogenide holey fibres from GeGaSbS glass," Mater. Res. Bull. **41**, 1303 – 1309 (2006).

16. J. C. Knight, J. Broeng, T. A. Birks, and P. S.-J. Russell, "Photonic band gap guidance in optical fibers," Science **282**, 1476–1478 (1998).

17. A. Argyros, T. Birks, S. Leon-Saval, C. M. Cordeiro, F. Luan, and P. S. J. Russell, "Photonic bandgap with an index step of one percent," Opt. Express **13**, 309–314 (2005).

18. J. D. Joannopoulos, S. G. Johnson, R. D. Meade, and J. N. Winn, *Photonic Crystals: Molding the Flow of Light*, 2nd ed. (Princeton Univ. Press, 2008).

19. M. Soljačić, S. G. Johnson, S. Fan, M. Ibanescu, E. Ippen, and J. D. Joannopoulos, "Photonic-crystal slow-light enhancement of non-linear phase sensitivity," J. Opt. Soc. Am. B **19**, 2052–2059 (2002).

20. Y. L. Hoo, W. Jin, C. Shi, H. L. Ho, D. N. Wang, and S. C. Ruan, "Design and Modeling of a Photonic Crystal Fiber Gas Sensor," Appl. Opt. **42**, 3509–3515 (2003).

21. J. B. Jensen, L. H. Pedersen, P. E. Hoiby, L. B. Nielsen, T. P. Hansen, J. R. Folkenberg, J. Riishede, D. Noordegraaf, K. Nielsen, A. Carlsen, and A. Bjarklev, "Photonic crystal fiber based evanescent-wave sensor for detection of biomolecules in aqueous solutions," Opt. Lett. **29**, 1974–1976 (2004).

22. T. Ritari, J. Tuominen, H. Ludvigsen, J. Petersen, T. Sørensen, T. Hansen, and H. Simonsen, "Gas sensing using air-guiding photonic bandgap fibers," Opt. Express **12**, 4080–4087 (2004).

23. S. Konorov, A. Zheltikov, and M. Scalora, "Photonic-crystal fiber as a multifunctional optical sensor and sample collector," Opt. Express **13**, 3454–3459 (2005).

24. J. Limpert, T. Schreiber, S. Nolte, H. Zellmer, T. Tunnermann, R. Iliew, F. Lederer, J. Broeng, G. Vienne, A. Petersson, and C. Jakobsen, "High-power air-clad large-mode-area photonic crystal fiber laser," Opt. Express **11**, 818–823 (2003).

25. W. Wadsworth, R. Percival, G. Bouwmans, J. Knight, and P. Russell, "High power air-clad photonic crystal fibre laser," Opt. Express **11**, 48–53 (2003).

26. F. Benabid, J. C. Knight, G. Antonopoulos, and P. S. J. Russell, "Stimulated Raman Scattering in Hydrogen-Filled Hollow-Core Photonic Crystal Fiber," Science **298**, 399–402 (2002).

27. J. McMillan, X. Yang, N. Panoiu, R. Osgood, and C. Wong, "Enhanced stimulated Raman scattering in slow-light photonic crystal waveguides," Opt. Lett. **31**, 1235–1237 (2006).

28. M. Soljačić, E. Lidorikis, M. Ibanescu, S. Johnson, J. Joannopoulos, and Y. Fink, "Optical bistability and cutoff solitons in photonic bandgap fibers," Opt. Express **12**, 1518–1527 (2004).

29. M. Notomi, K. Yamada, A. Shinya, J. Takahashi, and I. Yokohama, "Extremely large group-velocity dispersion of line-defect waveguides in photonic crystal slabs," Phys. Rev. Lett. **87**, 253,902 (2001).

30. Y. Vlasov, M. O'Boyle, H. Hamann, and S. McNab, "Active control of slow light on a chip with photonic crystal waveguides," Nature **438**, 65–69 (2005).

31. M. Settle, R. Engelen, M. Salib, A. Michaeli, L. Kuipers, and T. Krauss, "Flatband slow light in photonic crystals featuring spatial pulse compression and terahertz bandwidth," Opt. Express **15**, 219–226 (2007).

32. T. Baba, "Slow light in photonic crystals," Nature Photonics **2**, 465–473 (2008).

33. A. Bamberger and A. S. Bonnet, "Mathematical Analysis of the Guided Modes of an Optical Fiber," J. Math. Anal. **21**, 1487–1510 (1990).

34. C. Jiang, M. Ibanescu, J. Joannopoulos, and M. Soljacic, "Zero–group-velocity modes in longitudinally uniform waveguides," Appl. Phys. Lett. **93**, 241,111 (2008).

35. T. A. Birks, J. C. Knight, and P. S. Russell, "Endlessly single-mode photonic crystal fiber," Opt. Lett. **22**, 961–963 (1997).

36. M. Ibanescu, S. G. Johnson, M. Soljačić, J. D. Joannopoulos, Y. Fink, O. Weisberg, T. D. Engeness, S. A. Jacobs, and M. Skorobogatiy, "Analysis of mode structure in hollow dielectric waveguide fibers," Phys. Rev. E **67**, 046,608 (2003).

37. M. Soljačić, M. Ibanescu, S. G. Johnson, J. D. Joannopoulos, and Y. Fink, "Optical bistability in axially modulated OmniGuide fibers," Opt. Lett. **28**, 516–518 (2003).

38. R. Chern, C. Chang, C. Chang, and R. Hwang, "Large full band gaps for photonic crystals in two dimensions computed by an inverse method with multigrid acceleration," Phys. Rev. E **68**(026704) (2003).

39. M. Yan and P. Shum, "Improved air-silica photonic crystal with a triangular airhole arrangement for hollow-core photonic bandgap fiber design," Opt. Lett. **30**, 1920–1922 (2005).

40. S. G. Johnson and J. D. Joannopoulos, "Block-iterative frequency-domain methods for Maxwell's equations in a planewave basis," Opt. Express **8**, 173–190 (2001).

41. T. Inui, Y. Tanabe, and Y. Onodera, *Group theory and its applications in physics* (Springer, 1990).

42. H. Kim, M. Digonnet, G. Kino, J. Shin, and S. Fan, "Simulations of the effect of the core ring on surface and air-core modes in photonic bandgap fibers," Opt. Express **12**, 3436–3442 (2004).

43. J. West, C. Smith., N. Borrelli, D. Allan, and K. Koch, "Surface modes in air-core photonic band-gap fibers," Opt. Express **12**, 1485–1496 (2004).

44. K. Saitoh, N. Mortensen, and M. Koshiba, "Air-core photonic band-gap fibers: The impact of surface modes," Opt. Express **12**, 394–400 (2004).

45. S. G. Johnson, M. Ibanescu, M. Skorobogatiy, O. Weisberg, T. D. Engeness, M. Soljačić, S. A. Jacobs, J. D.

Joannopoulos, and Y. Fink, "Low-loss asymptotically single-mode propagation in large-core OmniGuide fibers," Opt. Express **9**, 748–779 (2001).

46. S. Johnson, P. Bienstman, M. Skorobogatiy, M. Ibanescu, E. Lidorikis, and J. Joannopoulos, "Adiabatic theorem and continuous coupled-mode theory for efficient taper transitions in photonic crystals," Phys. Rev. E **66**(066608) (2002).

47. M. Povinelli, S. Johnson, and J. Joannopoulos, "Slow-light, band-edge waveguides for tunable time delays," Opt. Express **13**, 7145–7159 (2005).

48. A. Oskooi, L. Zhang, Y. Avniel, and S. Johnson, "The failure of perfectly matched layers, and towards their redemption by adiabatic absorbers," Opt. Express **16**, 11,376–11,392 (2008).

49. A. Mutapcic, S. Boyd, A. Farjadpour, S. Johnson, and Y. Avniel, "Robust design of slow-light tapers in periodic waveguides," Engineering Optimization **41**, 365–384 (2009).

50. E. Magi, P. Steinvurzel, and B. Eggleton, "Tapered photonic crystal fibers," Opt. Express **12**, 776–784 (2004).

51. B. Lee, J. Eom, J. Kim, D. Moon, U.-C. Park, and G.-H. Yang, "Photonic crystal fiber coupler," Opt. Lett. **27**, 812–814 (2002).

52. A. Mekis and J. Joannopoulos, "Tapered Couplers for Efficient Interfacing Between Dielectric and Photonic Crystl Waveguides," J. Lightwave Tech. **19**, 861–865 (2001).

53. A. Talneau, P. Lalanne, M. Agio, and C. Soukoulis, "Low-reflection photonic-crstal taper for efficient coupling between guide sections of arbitrary widths," Opt. Lett. **27**, 1522–1524 (2002).

54. D. Mori and T. Baba, "Wideband and low dispersion slow light by chirped photonic crystal coupled waveguide," Opt. Express **13**, 9398–9408 (2005).

1. Introduction

Photonic-crystal holey fibers have been of great interest for a variety of different applications, mainly using silica or polymers with low index contrasts ($\sim 1.5 : 1$) [1]. Researchers have also studied photonic-crystal fiber-like geometries with high index contrast materials (eg. Si or GaAs, index ~ 3.4) [2–8] and shown that they support interesting zero–group-velocity modes [3], but to our knowledge such modes have not been described for fibers made of easily drawable materials. In this work, we demonstrate the possibility of obtaining zero–group-velocity modes in uniform fiber geometries using chalcogenide glasses (index ~ 2.8 [9]), which have proven amenable to drawn microstructured fibers [10–15]. Holey fibers, formed by a lattice of air holes in the fiber cross section, are best known for supporting "finger-like" band gaps opening towards the high-frequency regime, which can open even for arbitrarily low index contrasts [1, 2, 16–18]. However, these gaps close before reaching a zero propagation constant β, and the guided modes that they support have all been found to have nonzero group velocity. If the index contrast is high enough to support a complete band gap for all polarizations in *two* dimensions, however, then the resulting *three* dimensional holey fiber has a gap extending from $\beta = 0$ to some nonzero β. Although such gaps appear in some earlier work for very high index contrasts (3.3–3.5:1), [2–8] here we point out that they are attainable in lower-contrast glassy materials (chalcogenides). Moreover, we argue that the key advantage of these gaps is that they can support guided fiber modes that have a zero group velocity at $\beta = 0$. The slow-light modes close to the zero-velocity band edge should enhance a wide variety of nonlinear phenemona and material interactions [18, 19], such as fiber-based sensors [20–23], fiber lasers [24, 25], or Raman scattering [26, 27], and the band edge should also support gap solitons [28]. Numerous experiments have demonstrated slow-light effects in planar optical devices [27, 29–32]. One simple structure that has a complete two-dimensional (2d) gap for chalcogenide/air index contrast is a triangular lattice of circular air holes. In this paper, we employ a modification of this structure that is optimized to have a slightly larger gap, but either structure (and any future complete-gap 2d designs) creates well-localized zero–group-velocity fiber modes.

Let us first review the basic terminology and characteristics of holey fibers [1, 18], and the origin of the gaps and zero–group-velocity modes in this paper. The propagating modes of a fiber with a constant permittivity cross-section $\varepsilon(x,y)$ can be described as some xy electric field pattern $\mathbf{E}(x,y)$ multiplied by $e^{i(\beta z - \omega t)}$, where β is the propagation constant and ω is the frequency. A holey fiber consists of a periodic cladding (usually a triangular lattice of air holes),

as well as a core (solid or hollow) that breaks the periodicity and supports guided modes. The dispersion relation, the plot of $\omega(\beta)$ for all solutions, can be divided into several regions (as in Figs. 1 and 2). First, there is a continuous (shaded) region, the light cone, consisting of all cladding (non-guided) modes that can propagate in the cladding far from the core. There are also regions of (β, ω) that have no cladding modes: band gaps within the light cone, which can confine gap-guided modes, and also an empty space below the light cone that can confine index-guided modes. The guided modes, exponentially localized to the vicinity of the core, appear as discrete bands $\omega_n(\beta)$ within the gaps and/or under the light cone. (Technically, in a finite-size fiber the gap-guided modes are leaky, but as this leakage rate decreases exponentially with the periodic cladding thickness it can be made negligible in practical contexts.) In order to confine light in an air core, the gaps and guided modes must lie above the light line $\omega = c\beta$ of air (since modes below the light line of air are evanescent in air regions). Normally, these guided bands are monotonically increasing, corresponding to a positive group velocity $d\omega/d\beta$ (and there is a proof that this is always the case for index-guided modes with a homogeneous cladding [33]). Zero group velocity (standing-wave modes) typically occurs only at values of β that have $z \to -z$ reflection symmetry (with rare exceptions [3, 34]), which in a uniform–cross-section fiber only occurs at $\beta = 0$. Index-guided modes are not possible at $\beta = 0$ (they become rapidly more weakly confined as $\beta \to 0$), so one must consider bandgap-guided modes. Unfortunately, the typical gaps that arise in holey fibers have their origin in the $\beta \to \infty$ limit (where the field patterns approximate those of a 2d metallic system [18, 35]), and are observed to close well before $\beta = 0$ is reached. The $\beta = 0$ point corresponds to a *two*-dimensional photonic crystal with in-plane propagation, whose modes can be decomposed into TE ($\mathbf{E}$ in xy plane) and TM ($\mathbf{E}$ in z direction) polarizations [18]. Typically, low-contrast materials such as silica/air will have a gap only for one of these polarizations (e.g. TE for air holes) [18]. Such a single-polarization 2d gap is not useful for guiding modes in a fiber, because the TE/TM distinction disappears for $\beta \neq 0$ and hence a single-polarization gap disappears [18]. On the other hand, if one can obtain an overlapping TE/TM gap at $\beta = 0$, which typically requires higher index contrasts, then it should be expected to persist for a nonzero range of β, even after the TE/TM distinction disappears [2–8]. We demonstrate that this, in fact, occurs, for index contrasts attainable in chalcogenide glasses that have been used for fiber drawing [10–15], contrary to some previous suggestions [2]. The resulting gap around $\beta = 0$ therefore supports guided modes that attain zero group velocity as $\beta \to 0$. In practice, one does not operate at the zero-velocity point itself, but rather at nearby frequencies, so that by operating closer and closer to the zero-velocity band edge one can make the group velocity of light arbitrarily small in principle (at the expense of bandwidth and greater sensitivity to absorption and other loss, as discussed below).

Several other mechanisms have been proposed for creating zero–group-velocity modes in fibers. Bragg fibers, consisting of concentric rings of two or more materials forming a one-dimensional photonic crystal, have a gap originating at $\beta = 0$ [1, 18] and consequently their guided modes attain zero group velocity at this point. (Although Bragg fibers do not have a complete 2d gap, this is compensated for by the rotational symmetry which eliminates modes propagating in the azimuthal direction at large radii [18].) These fiber modes resemble those of hollow metallic waveguides [36], which also have zero group velocity at their cutoff frequencies. However, Bragg fibers require two solid materials in the cladding, which makes fabrication more challenging, while metallic waveguides become lossy at infrared frequencies. With a traditional core-clad fiber or with a holey fiber, zero group velocity can instead be attained by periodic modulation of the structure along the axial direction. For example, a fiber Bragg grating is formed by a weak modulation of the refractive index "burned" in by a photorefractive effect. Because this index modulation is typically much less than 1%, however, the low group-velocity bandwidth is small in fiber Bragg gratings. Furthermore, one can only modu-
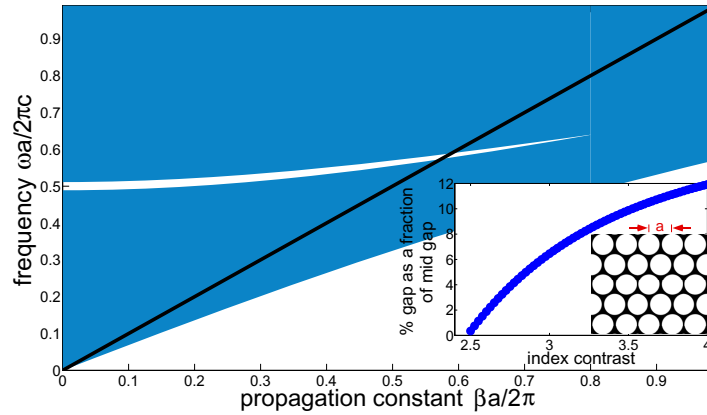
Fig. 1. Projected band diagram (frequency ω vs. propagation constant β), for a triangular lattice of holes (inset). Inset: optimized 2d ($\beta = 0$) gap size vs. index contrast.
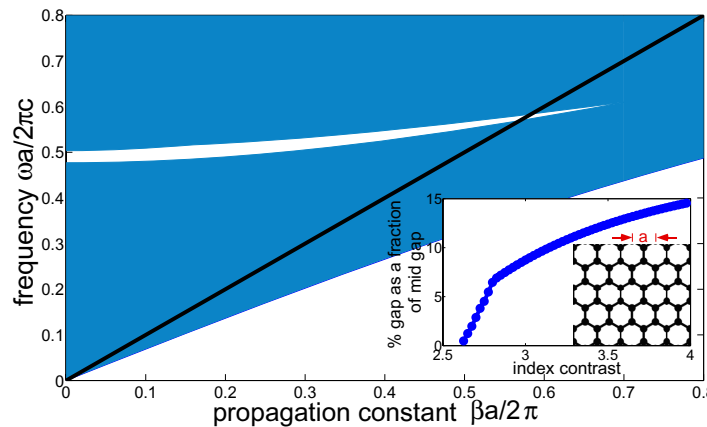

Fig. 2. Projected band diagram (frequency ω vs. propagation constant β), for a triangular lattice of hexagonal-shaped holes (inset). Inset: optimized 2d ($\beta = 0$) gap size vs. index contrast.

late the index of a solid material, greatly reducing the grating effect for modes confined in an air core. It has been proposed that spherical particles could be introduced into an air core in order to create a periodic modulation [37], but such structures seem challenging to produce on large scales compared to drawn fibers. Previous work showed that semiconductor (silicon) index contrasts (3.5:1) could support zero-group velocity modes in fiber-like geometries [3], and here we underline the existence and utility of analogous modes with conventional fiber materials. Furthermore, our previous work demonstrated that such zero group-velocity modes can even be converted into backwards-wave and ultra-flat bands by careful tuning of the waveguide core [3], and we expect that similar phenomena should be possible in chalcogenide fibers and other lower-contrast materials.

2. Gaps and defect modes

One 2d photonic crystal structure that is well known to have a complete gap for sufficiently large index contrast is a triangular lattice (period a) of cylindrical air holes (radius r) in dielectric [18],
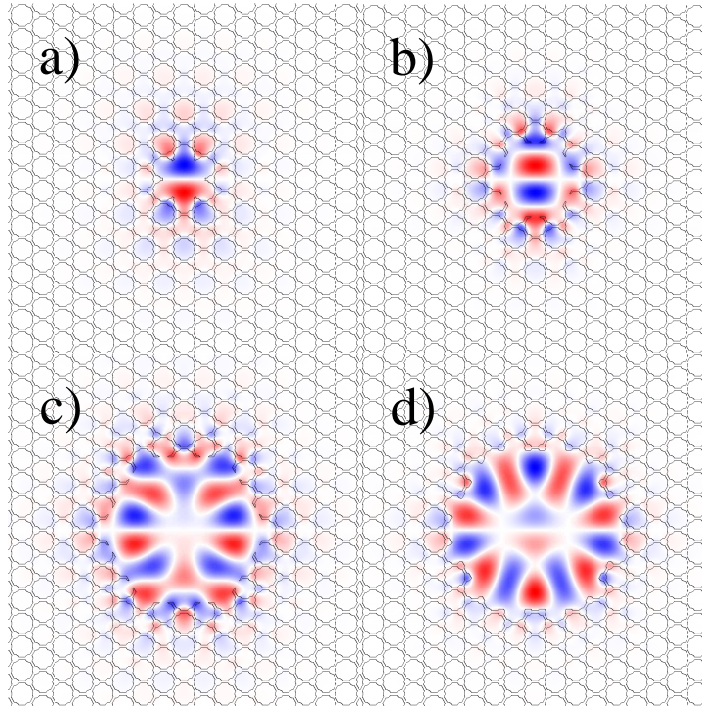
Fig. 3. Doubly-degenerate Γ_6 defect modes for a triangular lattice of hexagonal-shaped holes with periodicity a obtained by varying inscribed defect diameter of a hexagonal-shaped air core: a) $D = 1.6a$ (fundamental-like) b) $D = 3.2a$ c) $D = 6.2a$ d) $D = 6.76a$ (blue/white/red = negative/zero/positive).

similar to the geometry of many fabricated holey fibers [1]. This geometry with $r = 0.45a$ turns out to have a 4.4% complete gap at $\beta = 0$ for a refractive index of 2.8, chosen to correspond to that of a typical chalcogenide glass (e.g., As_2Se_3 at $\lambda = 1.5\mu m$ [9]). We also considered a slightly modified 2d photonic crystal consisting of a triangular lattice of dielectric rods in air connected by thin veins (resembling hexagonal-shaped holes) [38, 39]. The gap size was optimized over two parameters, rod radius and vein thickness, yielding a 5.4% gap-to-midgap ratio for a rod radius of $0.16a$ and a vein thickness of $0.2a$. The gap in this structure persisted for index contrasts as low as 2.6:1 (as shown in the inset of Fig. 2). The Maxwell eigenproblem was solved with an iterative (conjugate gradient) method in a planewave basis [40]. The resulting band diagrams, with gaps that extend over a range of nonzero β, are shown in Figs. 1 and 2. Since the modified structure of Fig. 2 has a slightly larger gap, we focus on this structure for the remainder of the paper; similar results can be obtained for the cylindrical-hole structure.

An air core is formed by removing some dielectric material, and here we do so by a hexagonal-shaped air core with an inscribed-circle diameter D in a $15a$ by $15a$ supercell. (This supercell is large enough that, for all guided modes considered here, the guided-mode field has decayed to negligible values by the edge of the supercell and hence the finite supercell size is irrelevant.) Depending on the core diameter D, different types of modes with varying symmetry and degrees of confinement can be localized [18]. We chose D to satisfy two criteria. First, the confined mode should be of the right symmetry to be excited by an incident planewave source—technically, this means that the mode is doubly degenerate and belongs to the Γ_6 representation of the sixfold (C_{6v}) symmetry group [41] of the hexagonal core. As D
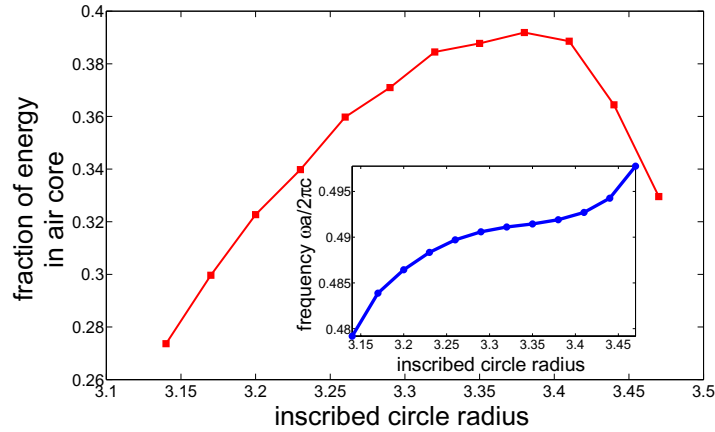
Fig. 4. Fraction of electric-field energy $\varepsilon|\mathbf{E}|^2$ in the hexagonal-shaped air core (as in Fig. 3) as a function of the core radius (radius of inscribed circle). Inset: frequency ω at $\beta = 0$ of guided mode vs. core radius.
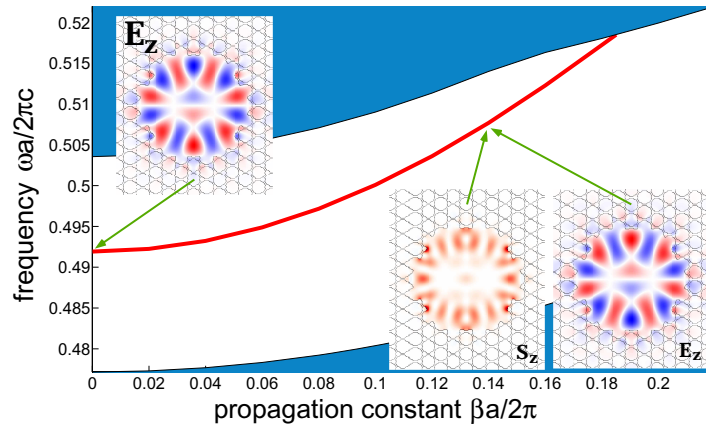

Fig. 5. Air-core guided mode in gap of Fig. 2, with insets showing electric-field E_z and Poynting vector S_z (blue/white/red = negative/zero/positive).

is varied, we obtain a variety of different Γ_6 defect modes, as shown in Fig. 3. For small D, we obtain fundamental-like fields patterns as in Fig. 3(a), whereas for larger D we obtain more complicated field patterns that are, however, better confined in the air core as in Fig. 3(d). For a given mode with strong air-core confinement, we then chose D to maximize the fraction of the electric-field energy ($\varepsilon|\mathbf{E}|^2$) in the air core at $\beta = 0$ (see Fig. 4) while also eliminating the influence of surface states [42–44]. This is desirable in air-core fiber applications to reduce absorption loss from the cladding and increase light-gas interactions. In particular, we chose the mode from Fig. 3(d) ($D = 6.76a$) for specificity, and the resulting structure is shown along with its dispersion relation in Fig. 5. The field profile (which is TM at $\beta = 0$) is still strongly confined at a non-zero axial wavevector ($\beta a/2\pi = 0.14$), as shown by the inset.

One source of loss is the material absorption in the cladding, which for bulk As_2Se_3 is about 36 dB/m at $\lambda = 1.5\ \mu$m [9]. For a guided mode in the hollow core, this absorption loss is suppressed by a factor of fc/v_gn, where f is the fraction of the electric-field energy in the cladding, v_g is the group velocity, and n is the cladding refractive index [18,45]. For the mode of Fig. 5
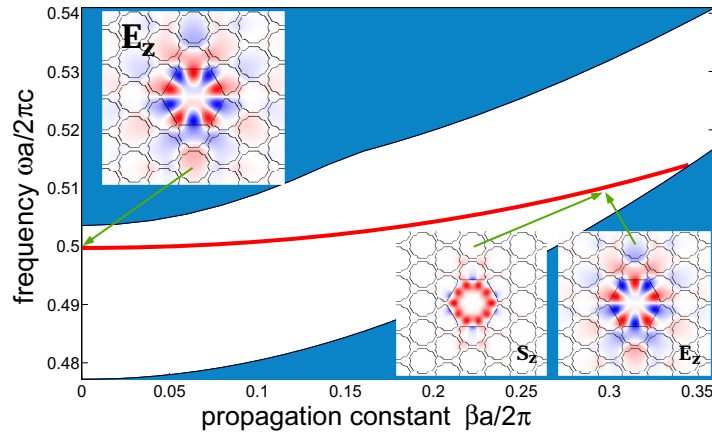
Fig. 6. Solid-core guided mode in gap of Fig. 2, with insets showing electric-field E_z and Poynting vector S_z (blue/white/red = negative/zero/positive).

at $\beta a/2\pi = 0.14$, where $v_g = 0.22c$ and $f = 0.19$, the absorption loss of the mode is therefore 11.1 dB/m, which is sufficient for short-distance fiber devices. Lower loss could be obtained by operating at a longer wavelength such as 3 or 10 μm, where the losses of chalcogenide are much lower while the index of refraction remains larger than 2.7 [9]. Another practical challenge in all slow-light structures is coupling from a non-slow source; one very general technique is a gradual "taper" transition to a higher-velocity waveguide [46–49], for example by gradually scaling the structure [50, 51] to a larger diameter to shift the band edge down to increase the group velocity at the operating ω. (Alternatively, rather than rescaling the whole structure, gradually *decreasing* the core diameter while keeping the cladding unchanged turns out to shift the band edge down in this geometry.) (Theoretically, a gradual enough transition can couple any pair of waveguides, no matter how different, with arbitrarily low reflection limited only by fabrication capabilities [46].) Minimization of reflections by proper design of couplers between very different modes of dielectric and photonic-crystal waveguides, including slow-light modes, has been studied elsewhere [46, 47, 49, 52–54], and a specific design for this fiber lies beyond the scope of this manuscript.

In contrast to air cores, solid (dielectric-filled) cores can be used to enhance interactions and nonlinearities with solid materials, such as for fiber lasers [24, 25]. Here, we form a small solid core by filling a hexagonal-shaped core ($D = 1.62a$) with dielectric. This confines a doubly-degenerate mode with an extremely flat dispersion relation, in addition to its zero–group-velocity point at $\beta = 0$, as shown in Fig. 6. This extreme flatness could potentially be transformed into a higher-order (e.g. quartic) band edge or even a concave backward-wave band-edge, via proper tuning of the solid core geometry [3].

3. Concluding remarks

Any holey photonic-crystal geometry with a complete gap for both polarizations in two dimensions can be used to obtain zero–group-velocity modes in a fiber geometry—our triangular lattice structure of hexagonal holes, here, is only one such example. An opportunity for future designs is to find complete gap structures with even lower index contrasts, in order that a wider range of materials become available for the fabrication of such slow-light devices. The ideal result would be a structure that has a complete 2d gap at silica/air index contrasts (1.5:1), but we are not currently aware of any geometry with this property.

Acknowledgements